PHOTONICS Research

Q-switching of waveguide lasers based on graphene/WS_2 van der Waals heterostructure

Ziqi Li,[1] Chen Cheng,[1] Ningning Dong,[2] Carolina Romero,[3] Qingming Lu,[4] Jun Wang,[2] Javier Rodríguez Vázquez de Aldana,[3] Yang Tan,[1] and Feng Chen[1,*]

[1]School of Physics, State Key Laboratory of Crystal Materials, Shandong University, Jinan 250100, China
[2]Key Laboratory of Materials for High-Power Laser, Shanghai Institute of Optics and Fine Mechanics, Chinese Academy of Sciences, Shanghai 201800, China
[3]Laser Microprocessing Group, Facultad Ciencias, Universidad de Salamanca, Salamanca 37008, Spain
[4]School of Chemistry and Chemical Engineering, Shandong University, Jinan 250100, China
*Corresponding author: drfchen@sdu.edu.cn

Received 2 June 2017; revised 9 July 2017; accepted 10 July 2017; posted 12 July 2017 (Doc. ID 297054); published 11 August 2017

We report on the operation of passively Q-switched waveguide lasers at 1 μm wavelength based on a graphene/WS_2 heterostructure as a saturable absorber (SA). The gain medium is a crystalline Nd:YVO_4 cladding waveguide produced by femtosecond laser writing. The nanosecond waveguide laser operation at 1064 nm has been realized with the maximum average output power of 275 mW and slope efficiency of 37%. In comparison with the systems based on single WS_2 or graphene SA, the lasing Q-switched by a graphene/WS_2 heterostructure SA possesses advantages of a higher pulse energy and enhanced slope efficiency, indicating the promising applications of van der Waals heterostructures for ultrafast photonic devices. © 2017 Chinese Laser Press

OCIS codes: (230.7370) Waveguides; (140.3540) Lasers, Q-switched; (130.0130) Integrated optics; (160.4236) Nanomaterials.

https://doi.org/10.1364/PRJ.5.000406

1. INTRODUCTION

As a basic component of integrated photonic circuits, an optical waveguide with diverse configurations could confine light propagation within dimensions of micrometer or submicrometer scales, offering a versatile platform for a broad range of applications [1,2]. A few well-developed techniques have been applied to fabricate various waveguide structures in dielectrics, such as ion/proton exchange [3], ion implantation [4], and femtosecond laser writing [5]. Among those developed fabrication techniques, femtosecond laser writing has been widely acknowledged as a powerful 3D micro-processing method to implement versatile photonic structures in a broad variety of materials since the pioneering work lead by Davis *et al.* in 1996 [6,7]. The focused femtosecond laser pulses can modify the refractive index permanently through a nonlinear process such as multiphoton absorption, avalanche ionization, and tunneling ionization [8]. The induced refractive-index modifications could be either positive ($\Delta n > 0$) or negative ($\Delta n < 0$), depending on the laser parameters and physical properties of the processed materials [9,10]. Recently, miniature and integratable laser sources based on the optical waveguide as gain media has attracted great research interest due to the outstanding lasing performances and the ease of integration with other optical devices. Waveguide lasers have been realized in both continuous-wave (CW) and pulsed operation regimes [11–13]. Benefiting from the compact geometry of the waveguide structures, superior lasing performances, e.g., reduced lasing thresholds and enhanced slope efficiencies, could be achieved with respect to the bulk laser systems [14]. Compared with the fiber laser system, the length of a waveguide cavity is much shorter, and the cavity volume is much smaller. The Nd:YVO_4 is one of most efficient gain media for solid-state laser systems owing to its outstanding features such as large stimulated emission cross section and strong broadband absorption [15]. For the pulsed laser operation, Q-switching by saturable absorbers (SAs) inside the laser cavity is one of the most common and efficient methods to generate nanosecond pulses, in which the SAs play an essential role in the ultrafast pulse generation.

In the past few years, graphene and other layered 2D materials, such as transition metal dichalcogenides (TMDCs, e.g., $MoSe_2$, WS_2), hexagonal boron nitride (*h*-BN), topological insulators (TIs, e.g., Bi_2Te_3), and black phosphorus (BP) have attracted tremendous interest from fundamental research as well as industries owing to their intriguing properties in a number of aspects [16–18]. Particularly, 2D materials possess unique and distinct optical properties such as polarization-dependent absorption and nonlinear optical absorption, which enable them as promising candidates in photonic applications [19]. Based on the waveguide configuration and nonlinear absorption properties of 2D materials, Q-switched lasers over

a variety of gain media have been widely reported [20–22]. Graphene has been demonstrated to be an ultra-broadband SA with remarkable optical properties such as linear optical absorption and ultrafast recovery time [23]. TMDCs exhibit strong light–matter interaction and ultrafast nonlinear absorption, which enable them as promising candidates for photonic applications [24]. To date, both graphene and WS_2 have been applied as suitable SA materials in Q-switched laser systems of waveguides [25,26] and other platforms [27,28]. In addition to the modification techniques implemented to equip desired functionalities of 2D materials [29–32], the ability to create heterostructures have opened up new possibilities for new physics and unique functionalities by combining distinct 2D materials with diverse properties into van der Waals heterostructures [33]. Monolayer WS_2 is a direct-bandgap semiconductor with a value of ∼1.8 eV [34] and is therefore a complement to graphene, which is a gapless semimetal. The graphene/WS_2 heterostructure has exhibited superior properties such as tunneling and thermionic transport, weak antilocalization effect, strong spin–orbit interaction, and ultrafast excitation transfer [35–38]. In optics, the layered heterostructures may introduce new features of SA, resulting in improved performances of lasing [39,40]. In this paper, in an Nd:YVO_4 waveguide platform, we implement the passively Q-switched waveguide lasers based on the SA of graphene/WS_2 heterostructure and compare the lasing characteristics of lasing Q-switched by separate graphene or WS_2 SA.

2. EXPERIMENTAL DETAILS AND DISCUSSION

The Nd:YVO_4 crystal (doped by 1 at. % Nd^{3+} ions) used in this work was cut into wafers of dimensions of 2(x) mm × 10(y) mm × 6(z) mm and was optically polished. The cladding waveguiding structures were fabricated by employing the laser facility of the Universidad de Salamanca, Spain, in which the Ti:sapphire regenerative amplifier (Spitfire, Spectra Physics) was utilized to generate linearly polarized 120 fs pulses at a central wavelength of 800 nm with 1 kHz repetition rate and 1 mJ maximum pulse energy. The pulse energy used to irradiate the sample was reduced by employing a calibrated neutral density filter placed after a half-wave plate and a linear polarizer to better control the incident energy. The sample was placed on a computer-controlled XYZ translation stage. The beam was focused through a 40× microscope objective (NA = 0.65) at certain depth beneath the largest sample surface (dimensions of 10 mm × 6 mm) at a depth ranges from 140 to 190 μm with a pulse energy of 10 μJ. During the irradiation, the sample was scanned at a constant velocity of 750 μm/s in the direction perpendicular to the laser polarization and the pulse propagation. The scanning direction was carefully aligned with the 10 mm long edge of the sample, thus producing a low refractive-index track along the sample. Under these conditions, the micromachining procedure was repeated at different positions of the sample, forming the desired circular geometry of the cladding waveguide with the diameter of 50 μm.

The graphene/WS_2 heterostructure used in this work was synthesized on the sapphire substrate (obtained from 6Carbon Technology). The WS_2 underlayer was synthesized on sapphire substrate directly via chemical vapor deposition (CVD) growth approach, and the upper-layer graphene was made by CVD and then transferred onto the bottom WS_2 layer. Figure 1(a) presents a schematic illustration of the vertically stacked heterobilayer of graphene/WS_2 on sapphire substrate. The samples of graphene and WS_2 used in this work were both fabricated on sapphire substrate by CVD technique and were characterized by Raman spectroscopy, as shown in Fig. 1(b), indicating the monolayer nature and good quality of the two samples compared with previous results [41,42]. Figure 1(d) demonstrates the measured room-temperature photoluminescence (PL) spectrum under the excitation of 532 nm laser in the same conditions. Compared with the PL peak of WS_2, a blueshift of the graphene/WS_2 heterostructure has been observed, which may be attributed to the released strain during the transfer process. Moreover, the PL intensity was strongly quenched in the graphene/WS_2 heterostructure, indicating the strong interlayer coupling between the two layers [36]. One possible explanation of the reduced PL intensity of the heterostructure is the ultrafast charge transfer process from WS_2 to the graphene, which hinders the recombination of photoexcited electron-hole pairs. To further evaluate the optical properties, the nonlinear optical performances of the three samples were investigated through the open-aperture Z-scan technique under 340 fs pulses operating at 1030 nm with the repetition of 100 Hz in the same configuration [43]. During the Z-scan experiments, the incident and transmitted powers were measured by two

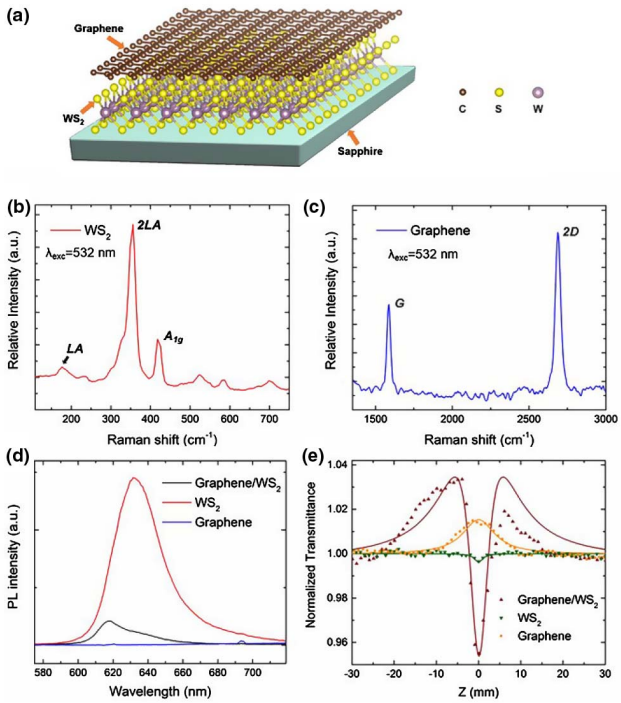

Fig. 1. (a) Schematic of graphene/WS_2 heterostructure on sapphire substrate. (b) Raman spectrum of the WS_2 sample. (c) Raman spectra of monolayer graphene. (d) PL spectrum measured from graphene/WS_2 heterostructure, WS_2, and graphene excited by 532 nm solid-state laser at room temperature. (e) Typical open-aperture Z-scan curves with normalized transmission as a function of sample position Z.

photodetectors, as the samples gradually moved along the laser propagation direction. Figure 1(e) shows the measured normalized transmission of three samples corresponding to the irradiance of 48.5 GW/cm^2 at $Z = 0$. It is worth noting that the linear absorption and thickness of the as-prepared heterostructure (~2.23 nm), WS_2 (0.8 nm), and graphene (0.4 nm) also have been taken into account in the calculation by employing the UV-Vis spectrophotometer and atomic force microscopy, in which the graphene/WS_2 heterostructure exhibited an enhanced linear absorption. By fitting the Z-scan data using the nonlinear absorption model [44,45], the heterostructure exhibited stronger nonlinear optical response with the combination of saturable absorption and multiphoton absorption. The fitted saturable intensity of graphene/WS_2 heterostructure was 4.72 GW/cm^2 and the nonlinear absorption coefficient (β) is measured to be 9.7×10^4 cm/GW, which is much higher than 1.33×10^3 cm/GW of WS_2, which is within a reasonable range under the same condition [43].

The Q-switched waveguide laser experiments were carried out utilizing the end-face coupling arrangement, as illustrated in Fig. 2. A linearly polarized light beam at 808 nm generated from a tunable CW Ti:sapphire laser (coherent MBR-PE) has been employed as the pump source and was set to be TE polarized by placing a linear polarizer. The pump laser was then coupled into the waveguide using a spherical convex lens with a focal length of 30 mm. The radius of the incident pump laser beam is approximately 0.75 nm. An input mirror (with the transmission of 98% at ~808 nm and the reflectivity >99% at ~1064 nm) and SA mirror (SAM) were adhered to the input and output end face of the waveguide, respectively, constructing the Fabry–Perot resonator with the Nd:YVO_4 waveguide gain media. The inset of Fig. 2 is the optical image of graphene/WS_2 heterostructure sample used in this work. The generated waveguide lasers were collected by utilizing a 20× microscope objective lens (NA = 0.4) and detected by an infrared CCD and an oscilloscope. A spectrometer with resolution of 0.2 nm was used to analyze the emission spectra of the pulsed laser beam from the waveguide.

In the laser system based on graphene/WS_2 heterostructure SA, the Q-switched laser emission spectrum from crystalline Nd:YVO_4 waveguide is depicted in Fig. 3(a). The central wavelength is 1064 nm with the FWHM bandwidth of ~0.8 nm, which corresponds to the main emission line of Nd^{3+} ion transition band $^4F_{3/2}$ to $^4I_{11/2}$ transition. As for WS_2 and graphene SAs, the same laser emission spectra have been achieved. The

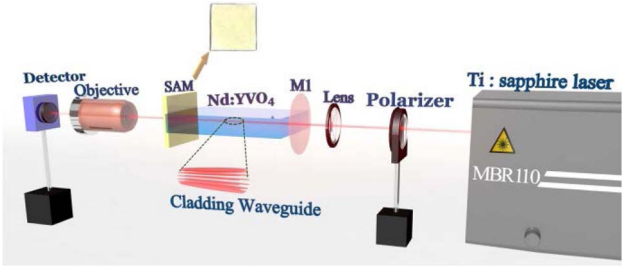

Fig. 2. Schematic of the experimental setup for Q-switched waveguide laser. Inset is an optical photograph of the graphene/WS_2 heterostructure on sapphire substrate.

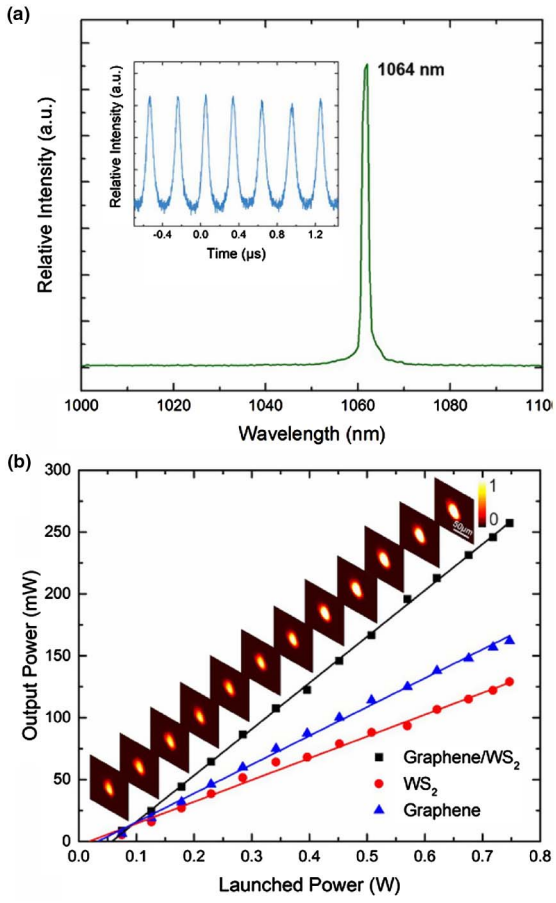

Fig. 3. Efficient Q-switched Nd:YVO_4 waveguide laser emission. (a) Emission spectrum of Q-switched waveguide laser modulated by graphene/WS_2 heterostructure. Insert is the pulse trains of Q-switched pulsed laser. (b) Output power versus the launched power. Inset is the evolution of measured near-field modal profile of the graphene/WS_2-based pulsed laser as the increase of launched power.

inset picture in Fig. 3(a) presents the Q-switched pulse laser trains under the pumping power of 0.53 W, with the average output power of 104 mW. Figure 3(b) depicts the measured average output power as a function of pumping power through linear fitting. As the increase of launched power, the output power of pulsed laser modulated by SAs of graphene/WS_2 heterostructure, WS_2, and graphene climbed to the maximums at 275, 184, and 231 mW with launched pump power of 747, 751, and 715 mW, corresponding to the slope efficiency of 37%, 17%, and 23%, respectively. Meanwhile, by linear fitting, the thresholds of the launched power of the pulsed laser oscillation were calculated to be 57.4, 18.1, and 33.2 mW, respectively. Compared with WS_2 and graphene, a Q-switched laser based on SAs of graphene/WS_2 heterostructure has much higher slope efficiency, which demonstrates the enhanced optical performance of this heterobilayer. The insert of Fig. 3(b) presents the measured near-field modal profile evolution of the pulsed laser oscillation as the increase of launched power when the SA is graphene/WS_2 heterostructure, in which the fundamental mode was achieved.

Figure 4 illustrates the dependence of pulse parameters (e.g., repetition rate, pulse duration, pulse energy, peak power)

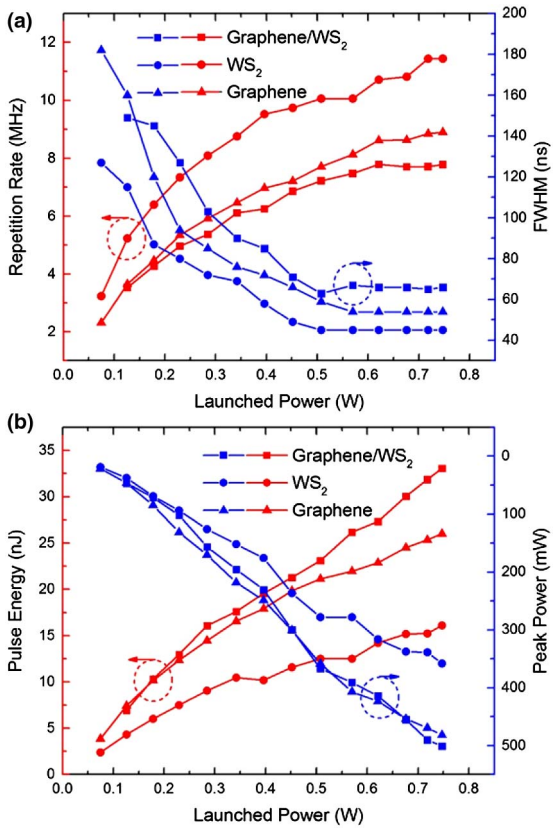

Fig. 4. Comparison of the parameters of pulsed laser *Q*-switched by SAs of graphene/WS heterostructure, WS_2, and graphene. (a) Repetition rate and pulse duration as a function of launched power. (b) Pulse energy and peak power as a function of launched power.

based on SAs of graphene/WS_2 heterostructure, WS_2, and graphene as a function of launched power in the same conditions. With the increase of the pump power, the repetition rate was tunable ranging from 3.528 to 7.777 MHz, 5.232 to 11.442 MHz, and 2.315 to 8.897 MHz, respectively. Simultaneously, the maximum single pulse energy reached 33.1 nJ (graphene/WS_2 heterostructure), 16.1 nJ (WS_2), and 26.0 nJ (graphene). By using graphene/WS_2 heterostructure as SA, the FWHM of the output laser was 149 ns and then rapidly decreased into a stable value of 66 ns. Moreover, the peak power ranges from 46.5 to 500.9 mW. Compared with WS_2 and graphene, a *Q*-switched laser based on SA of graphene/WS_2 heterostructure has superb performances with relatively higher pulse energy and peak power.

3. CONCLUSIONS

In conclusion, we have fabricated a cladding waveguide structure in the Nd:YVO_4 crystal and realized efficient passively *Q*-switched waveguide lasers modulated by using novel graphene/WS_2 heterostructure as an SA. The maximum output power was measured to be more than 275 mW with slope efficiency of 37%, corresponding to a single pulse energy of 33.1 nJ, of which higher pulse energy and enhanced slope efficiency were achieved by the comparison of WS_2 and graphene under the same configuration. The substrate effects of 2D layers with a different stacking sequence could be carried out in the future works. This work indicates that the layered graphene/WS_2 heterostructure could serve as promising SA materials for ultrafast photonic applications.

Funding. 111 Project of China (B13029); Strategic Priority Research Program of CAS (XDB16030700); Key Research Program of Frontier Science of CAS (QYZDB-SSW-JSC041); National Natural Science Foundation of China (NSFC) (11274203, 61522510); STCSM Excellent Academic Leader of Shanghai (17XD1403900).

REFERENCES

1. E. J. Murphy, *Integrated Optical Circuits and Components* (Marcel Dekker, 1999).
2. J. C. F. Matthews, A. Politi, A. Stefanov, and J. L. O'Brien, "Manipulation of multiphoton entanglement in waveguide quantum circuits," Nat. Photonics **3**, 346–350 (2009).
3. D. Kip, "Photorefractive waveguides in oxide crystals: fabrication, properties, and applications," Appl. Phys. B **67**, 131–150 (1998).
4. F. Chen, "Micro- and submicrometric waveguiding structures in optical crystals produced by ion beams for photonic applications," Laser Photon. Rev. **6**, 622–640 (2012).
5. F. Chen and J. R. Vázquez de Aldana, "Optical waveguides in crystalline dielectric materials produced by femtosecond-laser micromachining," Laser Photon. Rev. **8**, 251–275 (2014).
6. K. M. Davis, K. Miura, N. Sugimoto, and K. Hirao, "Writing waveguides in glass with a femtosecond laser," Opt. Lett. **21**, 1729–1731 (1996).
7. D. Choudhury, J. R. Macdonald, and A. K. Kar, "Ultrafast laser inscription: perspectives on future integrated applications," Laser Photon. Rev. **8**, 827–846 (2014).
8. B. C. Stuart, M. D. Feit, S. Herman, A. M. Rubenchik, B. W. Shore, and M. D. Perry, "Nanosecond-to-femtosecond laser-induced breakdown in dielectrics," Phys. Rev. B **53**, 1749–1761 (1996).
9. S. M. Eaton, H. Zhang, M. L. Ng, J. Z. Li, W. J. Chen, S. Ho, and P. R. Herman, "Transition from thermal diffusion to heat accumulation in high repetition rate femtosecond laser writing of buried optical waveguides," Opt. Express **16**, 9443–9458 (2008).
10. J. Burghoff, H. Hartung, S. Nolte, and A. Tünnermann, "Structural properties of femtosecond laser-induced modifications in $LiNbO_3$," Appl. Phys. A **86**, 165–170 (2007).
11. G. Palmer, S. Gross, A. Fuerbach, D. G. Lancaster, and M. J. Withford, "High slope efficiency and high refractive index change in direct-written Yb-doped waveguide lasers with depressed claddings," Opt. Express **21**, 17413–17420 (2013).
12. T. Calmano, A. G. Paschke, S. Müller, C. Kränkel, and G. Huber, "Curved Yb:YAG waveguide lasers, fabricated by femtosecond laser inscription," Opt. Express **21**, 25501–25508 (2013).
13. R. Mary, G. Brown, S. J. Beecher, F. Torrisi, S. Milana, D. Popa, T. Hasan, Z. P. Sun, E. Lidorikis, S. Ohara, A. C. Ferrari, and A. K. Kar, "1.5 GHz picosecond pulse generation from a monolithic waveguide laser with a graphene-film saturable output coupler," Opt. Express **21**, 7943–7950 (2013).
14. C. Grivas, "Optically pumped planar waveguide lasers, Part I: fundamentals and fabrication techniques," Prog. Quantum Electron. **35**, 159–239 (2011).
15. H. Yu, J. Liu, H. Zhang, A. A. Kaminskii, Z. Wang, and J. Wang, "Advances in vanadate laser crystals at a lasing wavelength of 1 micrometer," Laser Photon. Rev. **8**, 847–864 (2014).
16. A. K. Geim and K. S. Novoselov, "The rise of graphene," Nat. Mater. **6**, 183–191 (2007).
17. J. S. Ponraj, Z. Q. Xu, S. C. Dhanabalan, H. Mu, Y. Wang, J. Yuan, P. Li, S. Thakur, M. Ashrafi, K. McCoubrey, Y. Zhang, S. Li, H. Zhang, and Q. Bao, "Photonics and optoelectronics of two-dimensional materials beyond graphene," Nanotechnology **27**, 462001 (2016).
18. W. Tao, X. Zhu, X. Yu, X. Zeng, Q. Xiao, X. Zhang, X. Ji, X. Wang, J. Shi, H. Zhang, and L. Mei, "Black phosphorus nanosheets as a robust

delivery platform for cancer theranostics," Adv. Mater. **29**, 1603276 (2017).
19. F. Xia, H. Wang, D. Xiao, M. Dubey, and A. Ramasubramaniam, "Two-dimensional material nanophotonics," Nat. Photonics **8**, 899–907 (2014).
20. Y. Tan, H. Zhang, C. Zhao, S. Akhmadaliev, S. Zhou, and F. Chen, "Bi_2Se_3 *Q*-switched Nd: YAG ceramic waveguide laser," Opt. Lett. **40**, 637–640 (2015).
21. C. Cheng, H. Liu, Y. Tan, J. R. Vázquez de Aldana, and F. Chen, "Passively *Q*-switched waveguide lasers based on two-dimensional transition metal diselenide," Opt. Express **24**, 10385–10390 (2016).
22. C. Cheng, H. Liu, Z. Shang, W. Nie, Y. Tan, B. R. Rabes, J. R. Vázquez de Aldana, D. Jaque, and F. Chen, "Femtosecond laser written waveguides with MoS_2 as saturable absorber for passively *Q*-switched lasing," Opt. Mater. Express **6**, 367–373 (2016).
23. Q. Bao and K. P. Loh, "Graphene photonics, plasmonics, and broadband optoelectronic devices," ACS Nano **6**, 3677–3694 (2012).
24. Q. H. Wang, K. Kalantar-Zadeh, A. Kis, J. N. Coleman, and M. S. Strano, "Electronics and optoelectronics of two-dimensional transition metal dichalcogenides," Nat. Nanotechnol. **7**, 699–712 (2012).
25. R. He, J. R. Vázquez de Aldana, and F. Chen, "Passively *Q*-switched Nd: YVO_4 waveguide laser using graphene as a saturable absorber," Opt. Mater. **46**, 414–417 (2015).
26. Y. Tan, Z. Guo, L. Ma, H. Zhang, S. Akhmadaliev, S. Zhou, and F. Chen, "*Q*-switched waveguide laser based on two-dimensional semiconducting materials: tungsten disulfide and black phosphorous," Opt. Express **24**, 2858–2866 (2016).
27. J. Liu, S. Wu, Q. Yang, and P. Wang, "Stable nanosecond pulse generation from a graphene-based passively *Q*-switched Yb-doped fiber laser," Opt. Lett. **36**, 4008–4010 (2011).
28. J. Lin, Y. Hu, C. Chen, C. Gu, and L. Xu, "Wavelength-tunable Yb-doped passively *Q*-switching fiber laser based on WS_2 saturable absorber," Opt. Express **23**, 29059–29064 (2015).
29. Z. Li and F. Chen, "Ion beam modification of two-dimensional materials: characterization, properties, and applications," Appl. Phys. Rev. **4**, 011103 (2017).
30. Y. Tan, X. Liu, Z. He, Y. Liu, M. Zhao, H. Zhang, and F. Chen, "Tuning of interlayer coupling in large-area graphene/WSe_2 van der Waals heterostructure via ion irradiation: optical evidences and photonic applications," ACS Photon. **4**, 1531–1538 (2017).
31. C. R. Ryder, J. D. Wood, S. A. Wells, and M. C. Hersam, "Chemically tailoring semiconducting two-dimensional transition metal dichalcogenides and black phosphorus," ACS Nano **10**, 3900–3917 (2016).
32. L. Ma, Y. Tan, M. Ghorbani-Asl, R. Boettger, S. Kretschmer, S. Zhou, Z. Huang, A. V. Krasheninnikov, and F. Chen, "Tailoring the optical properties of atomically-thin WS_2 via ion irradiation," Nanoscale (2017), doi: 10.1039/C7NR02025B.
33. K. S. Novoselov, A. Mishchenko, A. Carvalho, and A. H. C. Neto, "2D materials and van der Waals heterostructures," Science **353**, aac9439 (2016).
34. Y. Ma, Y. Dai, M. Guo, C. Niu, J. Lu, and B. Huang, "Electronic and magnetic properties of perfect, vacancy-doped, and nonmetal adsorbed $MoSe_2$, $MoTe_2$ and WS_2 monolayers," Phys. Chem. Chem. Phys. **13**, 15546–15553 (2011).
35. T. Georgiou, R. Jalil, B. D. Belle, L. Britnell, R. V. Gorbachev, S. V. Morozov, Y.-J. Kim, A. Gholinia, S. J. Haigh, O. Makarovsky, L. Eaves, L. A. Ponomarenko, A. K. Geim, K. S. Novoselov, and A. Mishchenko, "Vertical field-effect transistor based on graphene-WS_2 heterostructures for flexible and transparent electronics," Nat. Nanotechnol. **8**, 100–103 (2013).
36. J. He, N. Kumar, M. Z. Bellus, H.-Y. Chiu, D. He, Y. Wang, and H. Zhao, "Electron transfer and coupling in graphene–tungsten disulfide van der Waals heterostructures," Nat. Commun. **5**, 5622 (2014).
37. E. C. T. O'Farrell, A. Avsar, J. Y. Tan, G. Eda, and B. Özyilmaz, "Quantum transport detected by strong proximity interaction at a graphene-WS_2 van der Waals interface," Nano Lett. **15**, 5682–5688 (2015).
38. S. Omar and B. J. van Wees, "Graphene-WS_2 heterostructures for tunable spin injection and spin transport," Phys. Rev. B **95**, 081404 (2017).
39. H. Mu, Z. Wang, J. Yuan, S. Xiao, C. Chen, Y. Chen, Y. Chen, J. Song, Y. Wang, Y. Xue, H. Zhang, and Q. Bao, "Graphene-Bi_2Te_3 heterostructure as saturable absorber for short pulse generation," ACS Photon. **2**, 832–841 (2015).
40. Z. Wang, H. Mu, J. Yuan, C. J. Zhao, Q. Bao, and H. Zhang, "Graphene-Bi_2Te_3 heterostructure as broadband saturable absorber for ultra-short pulse generation in Er-doped and Yb-doped fiber lasers," IEEE J. Sel. Top. Quantum Electron. **23**, 195–199 (2017).
41. A. C. Ferrari, J. C. Meyer, V. Scardaci, C. Casiraghi, M. Lazzeri, F. Mauri, S. Piscanec, D. Jiang, K. S. Novoselov, S. Roth, and A. K. Geim, "Raman spectrum of graphene and graphene layers," Phys. Rev. Lett. **97**, 187401 (2006).
42. A. Berkdemir, H. R. Gutierrez, A. R. Botello-Mendez, N. Perea-Lopez, A. L. Elias, C.-I. Chia, B. Wang, V. H. Crespi, F. Lopez-Urias, J.-C. Charlier, H. Terrones, and M. Terrones, "Identification of individual and few layers of WS_2 using Raman spectroscopy," Sci. Rep. **3**, 1755 (2013).
43. S. Zhang, N. Dong, N. McEvoy, M. O'Brien, S. Winters, N. C. Berner, C. Yim, Y. Li, X. Zhang, Z. Chen, L. Zhang, G. S. Duesberg, and J. Wang, "Direct observation of degenerate two-photon absorption and its saturation in WS_2 and MoS_2 monolayer and few-layer films," ACS Nano **9**, 7142–7150 (2015).
44. M. Sheik-Bahae, A. A. Said, T. H. Wei, D. J. Hagan, and E. W. Van Stryland, "Sensitive measurement of optical nonlinearities using a single beam," IEEE J. Quantum Electron. **26**, 760–769 (1990).
45. X. Zhang, A. Selkirk, S. Zhang, J. Huang, Y. Li, Y. Xie, N. Dong, Y. Cui, L. Zhang, W. J. Blau, and J. Wang, "MoS_2/carbon nanotube core-shell nanocomposites for enhanced nonlinear optical performance," Chemistry **23**, 3223 (2016).